Journal of Power Sources 252 (2014) 21–27

Contents lists available at ScienceDirect

Journal of Power Sources

journal homepage: www.elsevier.com/locate/jpowsour

Visible-light photocatalytic activity of Pt supported TiO_2 combined with up-conversion luminescence agent (Er^{3+}:$Y_3Al_5O_{12}$) for hydrogen production from aqueous methanol solution

Shuguang Li [a], Yuwei Guo [a,b], Lei Zhang [a], Jun Wang [a,*], Yun Li [a], Ying Li [a], Baoxin Wang [a]

[a] College of Chemistry, Liaoning University, Shenyang, Liaoning 110036, PR China
[b] Department of Chemistry, Baotou Normal College, Baotou 014030, PR China

HIGHLIGHTS

- The novel visible-light H_2 production photocatalysts (Er^{3+}:$Y_3Al_5O_{12}$/Pt−TiO_2) were prepared.
- Er^{3+}:$Y_3Al_5O_{12}$/Pt−TiO_2 can effectively perform visible-light photocatalytic H_2 production.
- A visible-light photocatalytic H_2 production process of Er^{3+}:$Y_3Al_5O_{12}$/Pt−TiO_2 was presented.

GRAPHICAL ABSTRACT

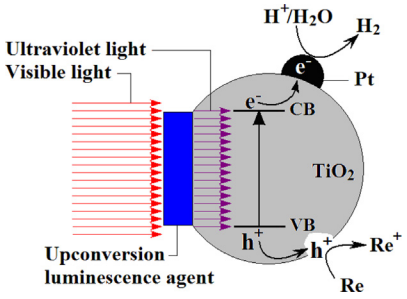

ARTICLE INFO

Article history:
Received 14 September 2013
Received in revised form
11 November 2013
Accepted 26 November 2013
Available online 8 December 2013

Keywords:
Pt-supported titanium dioxide
Up-conversion luminescence agent
Visible-light photocatalyst
Methanol splitting
Hydrogen production

ABSTRACT

In this paper, a high effective up-conversion luminescence agent (Er^{3+}:$Y_3Al_5O_{12}$) is synthesized by sol–gel method, and then its corresponding visible-light photocatalyst (Er^{3+}:$Y_3Al_5O_{12}$/Pt−TiO_2) is successfully prepared by direct mixing and calcination methods. For comparison, Er^{3+}:$Y_3Al_5O_{12}$, Pt−TiO_2 and Er^{3+}:$Y_3Al_5O_{12}$/Pt−TiO_2 are all characterized by X-ray diffractometer (XRD), scanning electron microscopy (SEM) and energy dispersive X-ray spectroscopy (EDX). At first, the up-conversion luminescence properties of Er^{3+}:$Y_3Al_5O_{12}$ are reviewed by excitation spectrum in visible-light region and emission spectrum in ultraviolet-light region. And then, under visible-light irradiation the visible-light photocatalytic activity of Er^{3+}:$Y_3Al_5O_{12}$/Pt−TiO_2 is examined through photocatalytic hydrogen production from aqueous methanol solution. Lastly, the influence factors such as Er^{3+}:$Y_3Al_5O_{12}$ and Pt−TiO_2 mole ratio, heat-treated temperature and heat-treated time on the visible-light photocatalytic hydrogen production activity of Er^{3+}:$Y_3Al_5O_{12}$/Pt−TiO_2 are studied. Particularly, Er^{3+}:$Y_3Al_5O_{12}$/Pt−TiO_2 with 6:100 M ratio heat-treated at 550 °C for 90 min shows the highest photocatalytic activity in hydrogen production from aqueous methanol solution.

1. Introduction

Along with the rapid population and economic growth in the coming decades, the world-wide energy consumption will be increased exponentially. Therefore, it is bound to further accelerate the depletion of non-renewable fuels. So the research about various substitute of energy gets more and more attention [1–3]. From the present study, it is widely believed that the solar energy is not only the most important basic energy of a variety of renewable energy, but also is the most abundant energy source [4,5]. Utilizing various semiconductor materials, the photocatalytic hydrogen production from water splitting offers an efficient way to capture solar energy

* Corresponding author. Tel.: +86 024 81917150; fax: +86 024 62202053.
E-mail addresses: wangjun888tg@126.com, wangjun890@sina.com (J. Wang).

0378-7753/$ – see front matter
http://dx.doi.org/10.1016/j.jpowsour.2013.11.100

and thus provide "greener" energy to solve the problem of serious energy crisis [6,7]. However, the choice of catalysts has always plagued the people for a long time. Fortunately, Fujishima and Honda discovered photoelectrochemical water splitting on a titanium dioxide (TiO_2) electrode in 1972 [8], since then it opened the prelude of photocatalytic hydrogen production from water splitting. TiO_2, as the most promising semiconductor photocatalyst, has been widely investigated on the conversion and degradation of inorganic or organic pollutants, but it is still far from being a perfect and ideal photocatalyst [9,10]. That is, due to the wide band gap ($E_{bg} \geq 3.2$ eV), TiO_2 can only utilize the ultraviolet-light that accounts for small proportion (<5.0%) of solar light for photocatalytic reaction. Therefore, by only using pure TiO_2 as catalyst the photocatalytic efficiency is too low to make full use of solar energy. In fact, it should be considered that for solving the energy problem it is necessary to try to utilize the visible-light (~48%) and near-infrared-light (~44%) of solar light for TiO_2 [11–14].

Recently, Wang et al. [15] reported a new approach assisted by hydrogen plasma to produce black titania with a crystalline core/amorphous shell structure (TiO_2@$TiO_{2-x}H_x$). This black titania reveals very strong visible-light and infrared-light absorption, which has yielded over an order of magnitude improvement in the effectiveness of solar-driven photocatalysis. Besides, it is also an ideal approach to combine TiO_2 with some up-conversion luminescence materials which can absorb visible-light and infrared-light in solar light and emit ultraviolet-light to make full use of solar energy for meeting the requirements of TiO_2 [16,17]. In recent years, we have been engaged in the study of TiO_2 combined with up-conversion luminescence agents to perform the visible-light photocatalytic degradation of organic pollutants [18–21]. Due to the use of the up-conversion luminescence agents, it not only greatly improves the photocatalytic degradation efficiency, but also shortens the reaction time. Since for TiO_2 there is a certain similarity in principle between the photocatalytic degradation and photocatalytic hydrogen production from water splitting, we think this method could also be applied to visible-light photocatalytic hydrogen production from water splitting.

So far, there are many kinds of up-conversion luminescence agents, for example, Er^{3+}:$YAlO_3$, Er^{3+}:$Y_3Al_5O_{12}$ and Yb^{3+}/Tm^{3+}:YF_3 etc., have been reported [22–24]. Among them, the Er^{3+}:$Y_3Al_5O_{12}$ is a typical of visible-to-ultraviolet up-conversion luminescence agent, which can generate one high-energy photon by absorbing two or more incident low-energy photons. In this process, the emission bands around 365 nm, 404 nm and 448 nm can be obtained under pumping at 654.0 nm. That is, the Er^{3+}:$Y_3Al_5O_{12}$ can absorb the red-light in visible-light region to emit ultraviolet-light and violet-light with high energy [25]. Since the solar light contains a continuous spectrum in visible-light and near-infrared regions, it can be used as a strong excitation light source. Hence, it can drive the Er^{3+}:$Y_3Al_5O_{12}$ emitting the ultraviolet-light which stimulates TiO_2 to carry out visible-light photocatalytic hydrogen production from water splitting. As a result, large-scale photocatalytic hydrogen production from water splitting using TiO_2 combined with Er^{3+}:$Y_3Al_5O_{12}$ as a novel photocatalyst under solar light irradiation is feasible in the future.

In this work, the up-conversion luminescence agent, Er^{3+}:$Y_3Al_5O_{12}$, was synthesized by sol–gel method and its corresponding visible-light photocatalysts, Er^{3+}:$Y_3Al_5O_{12}$/Pt–TiO_2, were successfully prepared by direct mixing and calcination methods. And then, under visible-light irradiation the TiO_2 nanoparticles combined with Er^{3+}:$Y_3Al_5O_{12}$ for visible-light photocatalytic hydrogen production was studied for the first time. The research results showed that the visible-light photocatalytic hydrogen production activity of TiO_2 could be significantly enhanced by the presence of Er^{3+}:$Y_3Al_5O_{12}$. In addition, the mechanism of up-conversion luminescence process of Er^{3+}:$Y_3Al_5O_{12}$ and the excitation principle of Er^{3+}:$Y_3Al_5O_{12}$/Pt–TiO_2 photocatalysts under visible-light irradiation were proposed.

2. Experimental procedure

2.1. Materials and reagents

Erbium oxide (Er_2O_3, 99.999%), yttrium oxide (Y_2O_3, 99.999%) and aluminum nitrate nonahydrate ($Al(NO_3)_3 \cdot 9H_2O$, analytical pure), citric acid ($C_6H_8O_7$, analytical pure) and nitric acid (HNO_3, analytical pure) (Veking Company, China) were used to synthesize the up-conversion luminescence agent (Er^{3+}:$Y_3Al_5O_{12}$). Titanium dioxide (TiO_2) nano-sized particles (20–30 nm, anatase phase, Sinopharm Chemical Regent Co., Ltd, China) were used to prepare the visible-light photocatalyst (Er^{3+}:$Y_3Al_5O_{12}$/TiO_2). hexachloroplatinic acid hexahydrate ($H_2PtCl_6 \cdot 6H_2O$, 97%, Sinopharm Chemical Regent Co., Ltd, China) was used as co-catalyst precursor for preparing Er^{3+}:$Y_3Al_5O_{12}$/Pt–TiO_2 photocatalysts [26,27]. Double distilled water (Millipore Corporation, USA) was buffered with methanol (CH_3OH, analytical pure, Veking Company, China), which acted as sacrificial agent. All chemicals were used without further purification.

2.2. Synthesis of up-conversion luminescence agent (Er^{3+}:$Y_3Al_5O_{12}$)

The up-conversion luminescence agent, Er^{3+}:$Y_3Al_5O_{12}$, was synthesized by sol–gel and calcination methods [28]. At first, $Y(NO_3)_3$ and $Er(NO_3)_3$ solutions were prepared by dissolving stoichiometric Y_2O_3 and Er_2O_3 into appropriate hot HNO_3 solution (about 60 °C), respectively. The prepared $Y(NO_3)_3$ and $Er(NO_3)_3$ solutions were mixed with $Al(NO_3)_3 \cdot 9H_2O$ while stirring magnetically, and the homogenous solution was obtained. Then the solid citric acid was added into the above mixture solution (mol ratio of citric acid: metal ion is 3:1). The solution was further stirred and heated at 50–60 °C until the transparent sol was successfully formed. Afterward, the transparent sol was heated at 80 °C for 24 h and became the gel. After being cooled in the air, the gel was ground into fine homogeneous powders. Subsequently, in order to remove residual organic components and nitrate ions the particles were calcined at 1100 °C for 2.0 h. At last, the sintered substance was taken out of the muffle furnace and allowed to cool down to the room temperature in atmosphere. Then, the desired white Er^{3+}:$Y_3Al_5O_{12}$ particles were obtained and stored for preparing the visible-light photocatalysts (Er^{3+}:$Y_3Al_5O_{12}$/Pt–TiO_2).

2.3. Preparation of visible-light photocatalysts (Er^{3+}:$Y_3Al_5O_{12}$/Pt–TiO_2)

The Er^{3+}:$Y_3Al_5O_{12}$/TiO_2 catalysts were prepared through the ultrasonic dispersion and liquid boiling method [29]. The Er^{3+}:$Y_3Al_5O_{12}$ and TiO_2 powders, whose mole ratios of Er^{3+}:$Y_3Al_5O_{12}$ and TiO_2 were adopted as 0:100, 1:100, 3:100, 6:100 and 12:100, respectively, were added into a 200 mL beaker filled with 30 mL deionized water and then adequately dispersed by ultrasound of 80 kHz frequency and 50 W output power for 30 min. The suspended liquid was heated to boiling point and kept at constant temperature for 30 min. After filtration and lavation, the separated deposit was put into a crucible and heated in a muffle furnace at the calefactive rate of 2.0 °C min^{-1}. The temperature was controlled at 450 °C, 550 °C and 650 °C, respectively, for different lengths of time (30 min, 60 min and 90 min, respectively). Finally, the Er^{3+}:$Y_3Al_5O_{12}$/TiO_2 catalysts were obtained.

Modification of Er^{3+}:$Y_3Al_5O_{12}$/TiO_2 with Pt as cocatalyst was accomplished by ultrasonic dispersion and liquid boiling method to

improve the activity of the photocatalysts [30]. Pt (0.1 wt %)-loaded Er^{3+}:$Y_3Al_5O_{12}$/TiO_2 were prepared by immersing Er^{3+}:$Y_3Al_5O_{12}$/TiO_2 particles in H_2PtCl_6 aqueous solution and then adequately dispersed by ultrasound of 80 kHz frequency and 50 W output power for 30 min. The suspended liquid was heated to boiling point and kept constant temperature for 30 min. After filtration and lavation, the separated powder was put into a crucible and heated in a constant temperature oven and then the temperature was controlled at 180 °C for 120 min. Finally, the Er^{3+}:$Y_3Al_5O_{12}$/Pt–TiO_2 catalysts were obtained. For comparison, the pure TiO_2 nanoparticles were also heat treated by the same procedure to obtain Pt–TiO_2catalyst.

2.4. Analytical method

The prepared Er^{3+}:$Y_3Al_5O_{12}$, Pt–TiO_2 and Er^{3+}:$Y_3Al_5O_{12}$/Pt–TiO_2 were characterized by powder X-ray diffraction (D-8, Brukeraxs, Germany) using Ni filtered Cu $K\alpha$ radiation in the range of 2θ from 10° to 70° and scanning electron microscopy (SEM, JEOL JSM-5610LV, Hitachi Corporation, Japan). The visible light excitation and ultraviolet light emission spectra of prepared Er^{3+}:$Y_3Al_5O_{12}$ were determined by Fluorescence spectrophotometer (FLSP920, Edinburgh Instruments, UK).

2.5. Visible-light photocatalytic hydrogen production experimental

The visible-light photocatalytic hydrogen production experiments were carried out in a 500 mL Pyrex reactor. The headspace of the reactor was connected to an inverted buret which is filled with water at atmospheric pressure, allowing the measurement of the evolved hydrogen gas. In the photocatalytic reactions for hydrogen production, Er^{3+}:$Y_3Al_5O_{12}$/Pt–TiO_2 powders (500 mg) were dispersed using a magnetic stirrer in methanol aqueous solution (5.0 wt %). The suspensions were purged with an argon flow for at least 30 min before visible-light irradiation in order to remove dissolved air. Then the suspensions were irradiated for 5.0 h using a 300 W xenon lamp (LX-300, Deruifeng hardware electrical appliance businesses, China). The irradiation wavelength was controlled by a combination of a cold mirror (CM-1) and a water filter ($350 < \lambda < 800$ nm). For visible-light irradiation, a cut off filter (L42) was fitted to the aforementioned light source ($420 < \lambda < 800$ nm). The formation of hydrogen was confirmed by injecting 0.5 mL of the reactor headspace gas in a gas chromatograph (GC-8A, MS-5A column, TCD, Ar Carrier, Shimadazu, Japan).

3. Results and discussion

3.1. XRD patterns, SEM and EDX images of Er^{3+}:$Y_3Al_5O_{12}$, Pt–TiO_2 and Er^{3+}:$Y_3Al_5O_{12}$/Pt–TiO_2

The XRD patterns of synthesized Er^{3+}:$Y_3Al_5O_{12}$ up-conversion luminescence agent and prepared Pt–TiO_2 and Er^{3+}:$Y_3Al_5O_{12}$/Pt–TiO_2 catalysts are all shown in Fig. 1. Obviously, the XRD pattern of synthesized Er^{3+}:$Y_3Al_5O_{12}$ (Fig. 1(a)) is similar to the JCPDS #33-0040 file of $Y_3Al_5O_{12}$ (Fig. 1(d)). It demonstrates that in the Er^{3+}:$Y_3Al_5O_{12}$ the $Y_3Al_5O_{12}$ has formed and the Er^{3+} entered the crystal lattice of $Y_3Al_5O_{12}$ replacing the partial Y^{3+} ion. In addition, the movement of the characteristic diffraction peak from $2\theta = 37.94°$ in Fig. 1(a) to $2\theta = 37.82°$ in Fig. 1(d) also indicates that a small quantity of Er^{3+} slightly changes the basic crystal structure of $Y_3Al_5O_{12}$. From Fig. 1(c) it can be found that, beside the normal characteristic diffraction peaks of TiO_2, the prepared Er^{3+}:$Y_3Al_5O_{12}$/Pt–TiO_2 catalysts also give the peaks of corresponding up-conversion luminescence agent (Er^{3+}:$Y_3Al_5O_{12}$). Being similar to that of Er^{3+}:$Y_3Al_5O_{12}$ (Fig. 1(a)), their main characteristic diffraction peaks are displayed at $2\theta = 18.12°$ (211), 33.36° (400), 42.58° (422), 46.62° (521) and 55.12° (532), respectively.

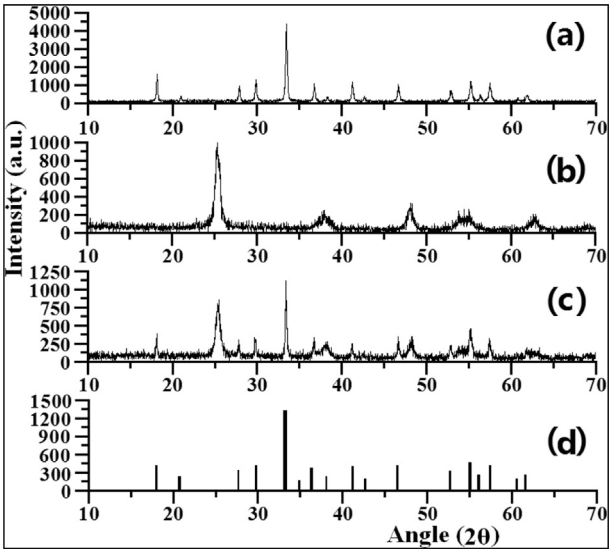

Fig. 1. XRD patterns of (a) Er^{3+}:$Y_3Al_5O_{12}$ (heat-treated at 1100 °C for 120 min), (b) Pt–TiO_2 (0.1 wt % Pt content heat-treated at 550 °C for 90 min), (c) Er^{3+}:$Y_3Al_5O_{12}$/Pt–TiO_2 (0.1 wt % Pt content and 6:100 Er^{3+}:$Y_3Al_5O_{12}$ and Pt–TiO_2 mole ratio heat-treated at 550 °C for 90 min) and (d) JCPDS #33-0040 file of $Y_3Al_5O_{12}$.

In addition, as can be seen in Fig. 1(c), according to the obvious characteristic diffraction peaks at $2\theta = 25.5°$ (101), 37.9° (004), 48.2° (200), 54.1° (105), 55.2° (211) and 62.8° (204), it can be estimated that the TiO_2 parts in Er^{3+}:$Y_3Al_5O_{12}$/Pt–TiO_2 catalysts mainly maintain the anatase crystal form. Besides, it also can be seen that the diffraction peaks at $2\theta = 27.5°$ (110) and $2\theta = 41.5°$ (111) which belong to the characteristic diffraction peaks of rutile phase appeared but very weak. Hence, the crystals form of TiO_2 part in Er^{3+}:$Y_3Al_5O_{12}$/Pt–TiO_2 catalysts heat-treated at 550 °C for 90 min can be identified as mixed crystal phase. The characteristic diffraction peaks of Pt from Fig. 1(b) and (c) cannot be found, which indicates that only 0.1 wt % Pt loaded on the surface of TiO_2 particles is not enough to generate the characteristic peaks in XRD patterns.

The SEM images of the Er^{3+}:$Y_3Al_5O_{12}$, Pt–TiO_2 and Er^{3+}:$Y_3Al_5O_{12}$/Pt–TiO_2 are all given in Fig. 2. From the image of Er^{3+}:$Y_3Al_5O_{12}$ depicted in Fig. 2(a), 50 nm homogeneous rod-shaped particles can be seen clearly. As seen in Fig. 2(b), there are a lot of morphology homogeneous gray elliptic balls and small white particles on it, it proves that Pt is deposited on TiO_2. In comparison, in Fig. 2(c) the Er^{3+}:$Y_3Al_5O_{12}$/Pt–TiO_2 catalysts displays an anomalous form with the average size the same as that of the Pt–TiO_2. Particularly, it can be seen that the small white flake particles on the surface of gray elliptic balls and some smaller white particles on them. These findings prove that Er^{3+}:$Y_3Al_5O_{12}$ has been combined with TiO_2 and Pt has been deposited on them.

The EDX spectra of synthesized Er^{3+}:$Y_3Al_5O_{12}$ up-conversion luminescence agent and prepared Er^{3+}:$Y_3Al_5O_{12}$/Pt–TiO_2 catalysts are both shown in Fig. 3. As displayed in Fig. 3(a), the results of EDX gives the peaks of Er, Y, Al, and O elements which compose the peaks of up-conversion luminescence agent. Besides, the atomic ratio of synthesized Er^{3+}:$Y_3Al_5O_{12}$ up-conversion luminescence agent is the same with the atomic ratio given in Fig. 3(a). From Fig. 3(b) it can be seen that the prepared catalysts contain Er^{3+}:$Y_3Al_5O_{12}$, Pt and TiO_2, the ratio of each material in the catalysts is the similar with the precursor solution.

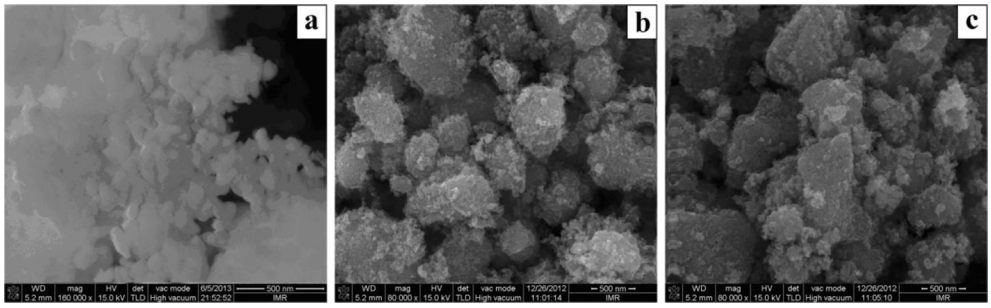

Fig. 2. SEM images of (a) Er^{3+}:$Y_3Al_5O_{12}$ (heat-treated at 1100 °C for 120 min), (b) Pt–TiO_2 (0.1 wt % Pt content heat-treated at 550 °C for 90 min) and (c) Er^{3+}:$Y_3Al_5O_{12}$/Pt–TiO_2 (0.1 wt % Pt content and 6:100 Er^{3+}:$Y_3Al_5O_{12}$ and Pt–TiO_2 mole ratio heat-treated at 550 °C for 90 min).

3.2. Visible-light excitation spectra and ultraviolet-light emission spectra of Er^{3+}:$Y_3Al_5O_{12}$

Visible-light excitation spectra and Ultraviolet-light emission spectra of Er^{3+}:$Y_3Al_5O_{12}$ were illustrated in Fig. 4(a). Considering the application of visible and infrared lights which accounts for more than 95% of solar light, the wavelength coverage from 400 nm to 800 nm was adopted for determining the excitation spectra. It can be seen that six typical excitation peaks located at 422 nm, 449 nm, 488 nm, 524 nm, 588 nm and 736 nm appear in excitation spectra and that a series of emission peaks located at 312 nm, 324 nm, 347 nm, 365 nm, 416 nm and 437 nm appear in emission spectra. According to the energy level scheme of Er^{3+}:$Y_3Al_5O_{12}$ shown in Fig. 4(b), these excitation peaks should be assigned to $^4I_{15/2} \rightarrow {}^4G_{11/2}$, $^4F_{7/2} \rightarrow {}^4D_{7/2}$, $^4I_{15/2} \rightarrow {}^2G_{9/2}$, $^4F_{7/2} \rightarrow {}^4D_{5/2}$, $^4I_{15/2} \rightarrow {}^4F_{7/2}$ and $^4S_{3/2} \rightarrow {}^4G_{11/2}$, respectively. Furthermore, these emission peaks should be assigned to $^2H_{9/2} \rightarrow {}^4I_{15/2}$, $^4D_{5/2} \rightarrow {}^4I_{11/2}$, $^4P_{3/2} \rightarrow {}^4I_{15/2}$, $^2H_{9/2} \rightarrow {}^4I_{11/2}$, $^2G_{9/2} \rightarrow {}^4I_{15/2}$ and $^4F_{7/2} \rightarrow {}^4I_{15/2}$, respectively [31–33]. Therefore, it can been found that the Er^{3+}:$Y_3Al_5O_{12}$ as up-conversion luminescence agent which can absorb visible and infrared lights in solar light and emit ultraviolet light, which can effectively activate TiO_2 to carry out photocatalytic hydrogen production. These findings prove that the TiO_2 combined with Er^{3+}:$Y_3Al_5O_{12}$ will be activated effectively by visible and infrared lights so as to enhance the effect of photocatalytic hydrogen production from aqueous methanol solution.

3.3. Photocatalytic activity comparison of Er^{3+}:$Y_3Al_5O_{12}$/Pt–TiO_2 and Pt–TiO_2 in visible-light photocatalytic hydrogen production

Fig. 5 shows the comparison of hydrogen production amounts catalyzed by Er^{3+}:$Y_3Al_5O_{12}$/Pt–TiO_2 and Pt–TiO_2 along with visible-light irradiation time. It can be found that the volumes of hydrogen production both increase gradually with the lengthening of visible-light irradiation time for two photocatalysts, but the volume by using Er^{3+}:$Y_3Al_5O_{12}$/Pt–TiO_2 catalysts is much more than that by using Pt–TiO_2 at any visible-light irradiation time. It can be considered that, because of the presence of Er^{3+}:$Y_3Al_5O_{12}$

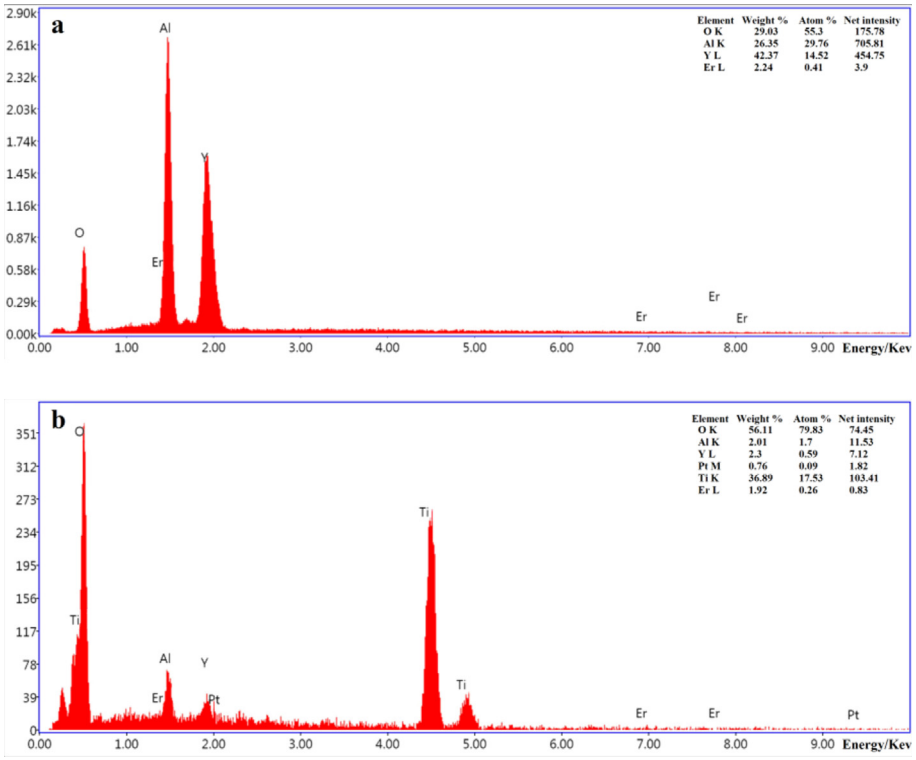

Fig. 3. EDX spectra of (a) Er^{3+}:$Y_3Al_5O_{12}$ (heat-treated at 1100 °C for 120 min) and (b) Er^{3+}:$Y_3Al_5O_{12}$/Pt–TiO_2 (0.1 wt % Pt content and 6:100 Er^{3+}:$Y_3Al_5O_{12}$ and Pt–TiO_2 mole ratio heat-treated at 550 °C for 90 min).

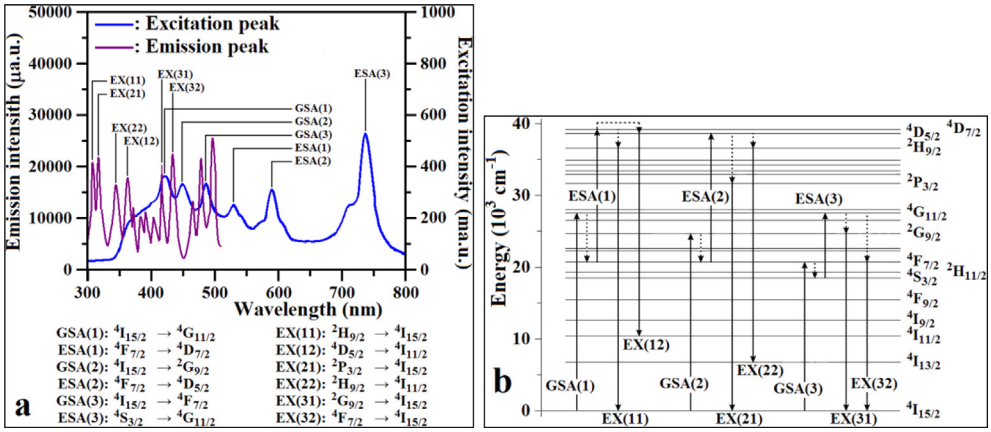

Fig. 4. (a) Characteristic visible-light excitation spectra and ultraviolet-light emission spectra of Er^{3+}:$Y_3Al_5O_{12}$ and (b) energy level scheme of Er^{3+}:$Y_3Al_5O_{12}$ and related transition processes.

possessing up-conversion luminescence effect from visible-light to ultraviolet-light, it can provide more ultraviolet-light to stimulate TiO_2 to carry out the photocatalytic hydrogen production. Furthermore, the applicable TiO_2 accounts for only 70% in the Er^{3+}:$Y_3Al_5O_{12}$/Pt–TiO_2 catalysts. When the effect of pure TiO_2 is just considered, the volumes of hydrogen production caused by Er^{3+}:$Y_3Al_5O_{12}$/Pt–TiO_2 and Pt–TiO_2 are 3.42 mL and 1.80 mL, respectively. It indicated that the presence of Er^{3+}:$Y_3Al_5O_{12}$ could obviously enhance the visible-light photocatalytic hydrogen production activity of the Pt–TiO_2 catalysts.

3.4. *The influence of visible-light irradiation intensity on photocatalytic hydrogen production effect of Er^{3+}:$Y_3Al_5O_{12}$/Pt–TiO_2*

The effect of irradiation intensity on the visible-light photocatalytic hydrogen production of Er^{3+}:$Y_3Al_5O_{12}$/Pt–TiO_2 is shown in Fig. 6. It can be found that the volumes of hydrogen production both increase along with the increase of visible-light irradiation intensity for Er^{3+}:$Y_3Al_5O_{12}$/Pt–TiO_2 and Pt–TiO_2. It indicates that the high-intensity visible-light irradiation is conducive to the photocatalytic hydrogen production of Er^{3+}:$Y_3Al_5O_{12}$/Pt–TiO_2 and Pt–TiO_2. Of course, under the same visible-light irradiation the volumes of hydrogen production of Er^{3+}:$Y_3Al_5O_{12}$/Pt–TiO_2 catalysts is much more than that of Pt–TiO_2 powder. It may be attributed to the fact that the Er^{3+}:$Y_3Al_5O_{12}$ offers more ultraviolet-light to TiO_2.

In fact, considering that the TiO_2 accounts for only 70% in the Er^{3+}:$Y_3Al_5O_{12}$/Pt–TiO_2 catalysts, due to the presence of Er^{3+}:$Y_3Al_5O_{12}$ the efficiency of hydrogen production by TiO_2 in Er^{3+}:$Y_3Al_5O_{12}$/Pt–TiO_2 catalysts is much higher than that of pure Pt–TiO_2 powder. For 10.0 mW cm^{-2} irradiation intensity, the calculated relative volume of hydrogen production of the same quality of Pt–TiO_2 in Er^{3+}:$Y_3Al_5O_{12}$/Pt–TiO_2 is up to 3.42 mL, and that the volume of hydrogen production of pure Pt–TiO_2 is only 1.80 mL. It also proves that the visible-light photocatalytic hydrogen production activity of the Er^{3+}:$Y_3Al_5O_{12}$/Pt–TiO_2 is much higher than that of Pt–TiO_2. These findings prompt us that the visible-light photocatalytic hydrogen production activity of the TiO_2 will be further improved if the coating method is adopted.

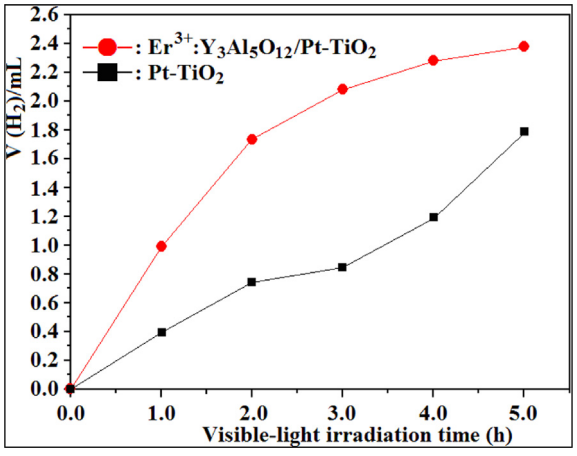

Fig. 5. Influences of visible-light irradiation time on photocatalytic hydrogen production effects of Pt–TiO_2 (0.1 wt % Pt content heat-treated at 550 °C for 90 min) and Er^{3+}:$Y_3Al_5O_{12}$/Pt–TiO_2 (0.1 wt % Pt content and 6:100 mol ratio Er^{3+}:$Y_3Al_5O_{12}$ and Pt–TiO_2 heat-treated at 550 °C for 90 min) as photocatalysts. (1.0 atmospheric pressure, 25 °C, 10.0 mW cm^{-2} (Xenon lamp) irradiation intensity, 500 mL total volume, 1000 mg L^{-1} catalyst and 5.0 wt % methanol sacrificial agent.)

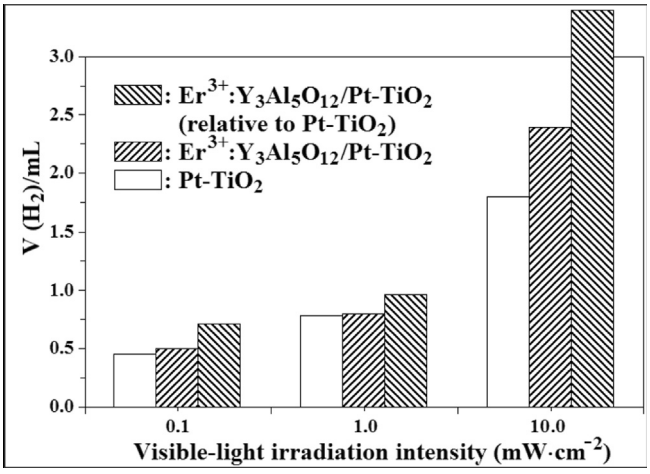

Fig. 6. Influences of visible-light irradiation intensity on photocatalytic hydrogen production effect of Pt–TiO_2 (0.1 wt % Pt content heat-treated at 550 °C for 90 min) and Er^{3+}:$Y_3Al_5O_{12}$/Pt–TiO_2 (0.1 wt % Pt content and 6:100 mol ratio Er^{3+}:$Y_3Al_5O_{12}$ and Pt–TiO_2 heat-treated at 550 °C for 90 min) as photocatalysts. (1.0 atmospheric pressure, 25 °C, 10.0 mW cm^{-2} (Xenon lamp) irradiation intensity, 5.0 h visible-light irradiation time, 500 mL total volume, 1000 mg L^{-1} catalyst and 5.0 wt % methanol as sacrificial agent.)

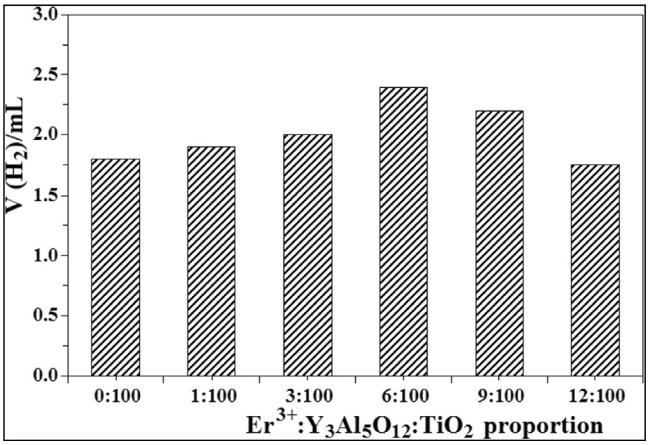

Fig. 7. Influence of Er^{3+}:$Y_3Al_5O_{12}$ and Pt–TiO_2 mole ratios on visible-light photocatalytic hydrogen production activity of Er^{3+}:$Y_3Al_5O_{12}$/Pt–TiO_2 (0.1 wt % Pt content heat-treated at 550 °C for 90 min) as photocatalyst under visible-light irradiation. (1.0 atmospheric pressure, 25 °C, 10.0 mW cm^{-2} (Xenon lamp) irradiation intensity, 5.0 h visible-light irradiation time, 500 mL total volume, 1000 mg L^{-1} catalyst and 5.0 wt % methanol sacrificial agent.)

3.5. The influence of Er^{3+}:$Y_3Al_5O_{12}$ and TiO_2 mole ratio on visible-light photocatalytic hydrogen production activity of Er^{3+}:$Y_3Al_5O_{12}$/Pt–TiO_2

Fig. 7 shows the relationship between the volume of photocatalytic hydrogen production of Er^{3+}:$Y_3Al_5O_{12}$/Pt–TiO_2 catalysts and mole ratio of Er^{3+}:$Y_3Al_5O_{12}$ and TiO_2 under visible-light irradiation [34,35]. It can be seen that the volume of photocatalytic hydrogen production increases with the increase of Er^{3+}:$Y_3Al_5O_{12}$ content (from 0:100 mol ratio to 6:100 mol ratio), and then slightly falls with further increases of Er^{3+}:$Y_3Al_5O_{12}$ content (from 6:100 mol ratio to 12:100 mol ratio). It indicates that the Er^{3+}:$Y_3Al_5O_{12}$ and TiO_2 mole ratio can affect the photocatalytic hydrogen production activity of Er^{3+}:$Y_3Al_5O_{12}$/Pt–TiO_2. The appropriate increase of Er^{3+}:$Y_3Al_5O_{12}$ content can offer much more ultraviolet-light to activate TiO_2 through up-conversion luminescence from visible-light and infrared-light to ultraviolet-light, which results in the increase of the volume of photocatalytic hydrogen production. However, because of using direct mixing method, the further increase of Er^{3+}:$Y_3Al_5O_{12}$ content relatively decreases the active surface of Er^{3+}:$Y_3Al_5O_{12}$/Pt–TiO_2 catalyst particles. It leads to the decrease of the volume of photocatalytic hydrogen production. It can be prompted that the coating method can avoid the decreases of the active surface of catalyst particles.

3.6. The influence of heat-treated temperature and heat-treated time on visible-light photocatalytic hydrogen production activity of Er^{3+}:$Y_3Al_5O_{12}$/Pt–TiO_2

In general, the heat-treated temperature and heat-treated time play an important role for the activity of many semiconductor photocatalysts. Particularly, for TiO_2, they decide the crystallization, particle size and surface properties as well as crystal form. Fig. 8(a) shows that low yield of hydrogen production using Er^{3+}:$Y_3Al_5O_{12}$/Pt–TiO_2 appears at 450 °C calcined temperature. This illuminates that the calcination at lower temperature leads to a lower combination grade between Er^{3+}:$Y_3Al_5O_{12}$ and TiO_2. That is, at 450 °C the Er^{3+}:$Y_3Al_5O_{12}$/Pt–TiO_2 composite is not well formed. At 550 °C, a high yield of hydrogen production is jointly attained. When the temperature is up to 650 °C, a mass of TiO_2 particles congregate together and the anatase phase of TiO_2 begin to transform into the rutile phase. The increase of the rutile phase debases the photocatalytic activity of Er^{3+}:$Y_3Al_5O_{12}$/Pt–TiO_2 catalysts.

Fig. 8(b) shows the effect of heat-treated time on the photocatalytic hydrogen production activity of Er^{3+}:$Y_3Al_5O_{12}$/Pt–TiO_2 catalysts. It can be found that the Er^{3+}:$Y_3Al_5O_{12}$/Pt–TiO_2 catalysts after 90 min heat-treated time present the highest photocatalytic activity. It can be inferred that the Er^{3+}:$Y_3Al_5O_{12}$ and TiO_2 particles cannot integrate well with short heat-treated time (30 min and 60 min), and the conglomeration of the Er^{3+}:$Y_3Al_5O_{12}$ particles may occur with long-playing heat-treated time (120 min). In addition, for TiO_2 at the sensitive temperature (phase transformation temperature from anatase to rutile), long time heat-treatment causes the generation of a large amount of rutile phase TiO_2. All these causes may reduce the visible-light photocatalytic hydrogen production activity of Er^{3+}:$Y_3Al_5O_{12}$/Pt–TiO_2 catalysts. So, in order to maintain a high photocatalytic activity, the proper heat-treated temperature and heat-treated time are necessary.

3.7. Possible visible-light photocatalytic hydrogen production mechanism and process

The mechanism of visible-light photocatalytic hydrogen production from aqueous methanol solution caused by Er^{3+}:$Y_3Al_5O_{12}$/Pt–TiO_2 catalysts under visible-light irradiation are shown in Fig. 9. On the basis of up-conversion luminescence feature of Er^{3+}:$Y_3Al_5O_{12}$, a tentative mechanism for the high visible-light photocatalytic hydrogen production activity of the Er^{3+}:$Y_3Al_5O_{12}$/Pt–TiO_2 catalysts was proposed. As up-conversion luminescence agent, the Er^{3+}:$Y_3Al_5O_{12}$ absorbs the visible-light in solar light and then emits ultraviolet-light, which can effectively excite the TiO_2 crystal. Under ultraviolet-light irradiation produced by Er^{3+}:$Y_3Al_5O_{12}$ with up-conversion luminescence effect, the

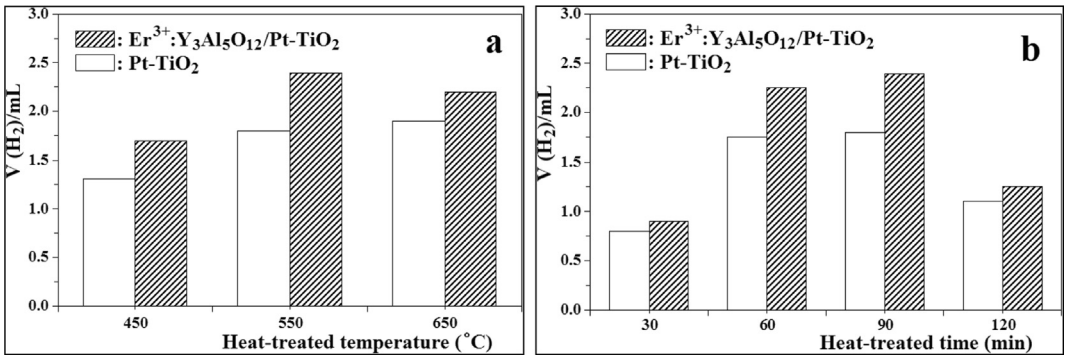

Fig. 8. Influences of (a) heat-treated temperature and (b) heat-treated time on visible-light photocatalytic hydrogen production activity of Er^{3+}:$Y_3Al_5O_{12}$/Pt–TiO_2 (0.1 wt% Pt content and 6:100 mol ratio Er^{3+}:$Y_3Al_5O_{12}$ and Pt–TiO_2 heat-treated at 550 °C for 90 min) under visible-light irradiation. (1.0 atmospheric pressure, 25 °C, 10.0 mW cm^{-2} (Xenon lamp) irradiation intensity, 5.0 h visible-light irradiation time, 500 mL total volume, 1000 mg L^{-1} catalyst and 5.0 wt % methanol sacrificial agent.).

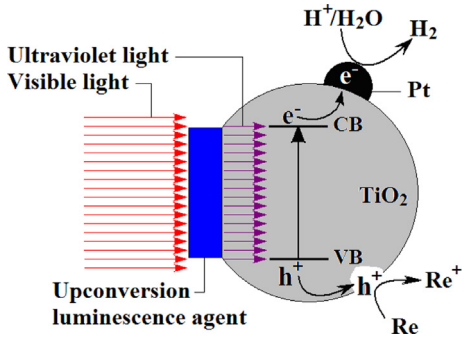

Fig. 9. Visible-light photocatalytic hydrogen production principle and process of Er^{3+}:$Y_3Al_5O_{12}$/Pt–TiO_2 under visible-light irradiation.

photogenerated electrons in the valence band (VB) of TiO_2 transit to the conduction band (CB), creating holes in the VB at the same time. The previous studies have shown that the photogenerated electrons in the CB of TiO_2 can be injected into Pt nanoparticles in a Pt–TiO_2 system [36]. The Pt deposited on the surface of TiO_2 can not only accept electrons acting as active sites for hydrogen production, but also decreases the recombination rate of photogenerated electrons and photogenerated holes, which increases the photocatalytic activity of Er^{3+}:$Y_3Al_5O_{12}$/TiO_2 catalysts. Due to the high reducibility, the electrons can restore the H^+ cations in the water to produce H_2. At the same time, the highly oxidative holes on VB of TiO_2 can oxidize the methanol as oxygen sacrificial agent to methanal or methane acid.

4. Conclusions

In this work, an effective up-conversion luminescence agent (Er^{3+}:$Y_3Al_5O_{12}$) was synthesized and then the corresponding visible-light photocatalysts (Er^{3+}:$Y_3Al_5O_{12}$/Pt–TiO_2) for visible-light photocatalytic hydrogen production were prepared by sol–gel and calcination methods. They were characterized by XRD, SEM, EDX, visible light excitation spectra and ultraviolet light fluorescence emission spectra. The visible-light photocatalytic hydrogen production activity from aqueous methanol solution was detected under visible-light irradiation. The results showed that the photocatalytic activity of TiO_2 in visible-light photocatalytic hydrogen production process could be enhanced obviously by adding up-conversion luminescence agent (Er^{3+}:$Y_3Al_5O_{12}$). Also, the photocatalytic activity of Er^{3+}:$Y_3Al_5O_{12}$/Pt–TiO_2 is related to the mole ratio of Er^{3+}:$Y_3Al_5O_{12}$ and TiO_2, heat-treated temperature and heat-treated time. For given experimental conditions, the prepared Er^{3+}:$Y_3Al_5O_{12}$/Pt–TiO_2 catalysts with 6:100 mol ratio heat-treated at 550 °C for 90 min display a highest visible-light photocatalytic hydrogen production activity. Perhaps, it provides a possible strategy for large-sale hydrogen production using solar energy in the future.

Acknowledgments

The authors greatly acknowledge the National Science Foundation of China (No. 21371084), Liaoning Provincial Department of Education Innovation Team Projects (No. LT2012001), Shenyang Science and Technology Plan Projects (No. F12-277-1-15) and Liaoning University "211" Engineering Construction Projects for financial support. The authors also thank our colleagues and other students for their participating in this work.

References

[1] A.J. Bard, G.M. Whitesides, R.N. Zare, F.W. McLafferty, Acc. Chem. Res. 28 (1995) 141–145.
[2] G. Hitoki, T. Takata, J.N. Kondo, M. Hara, H. Kobayashi, K. Domen, Chem. Commun. 16 (2002) 1698–1699.
[3] M. Anpo, M. Takeuchi, J. Catal. 216 (2003) 505–516.
[4] H.G. Kim, D.W. Hwang, J.S. Lee, J. Am. Chem. Soc. 126 (2004) 8912–8913.
[5] Y. Sasaki, H. Nemoto, K. Saito, A. Kudo, J. Phys. Chem. C 113 (2009) 17536–17542.
[6] K. Maeda, T. Takata, M. Hara, N. Saito, Y. Inoue, H. Kobayashi, K. Domen, J. Am. Chem. Soc. 127 (2005) 8286–8287.
[7] G.K. Mor, H.E. Prakasam, O.K. Varghese, K. Shankar, C.A. Grimes, Nano. Lett. 7 (2007) 2356–2364.
[8] A. Fujishima, K. Honda, Nature 238 (1972) 37–38.
[9] O. Carp, C.L. Huisman, A. Reller, Prog. Solid State Chem. 32 (2004) 42–90.
[10] Y.H. Ng, S. Ikeda, M. Matsumura, R. Amal, Energy Environ. Sci. 5 (2012) 9307–9318.
[11] X.B. Chen, S.S. Mao, Chem. Rev. 107 (2007) 2891–2959.
[12] A. Jirapat, K. Puangrat, S. Supapan, J. Hazard. Mater. 168 (2009) 253–261.
[13] J. Wang, D.N. Tafen, J.P. Lewis, Z. Hong, A. Manivannan, M. Zhi, M. Li, N. Wu, J. Am. Chem. Soc. 131 (2009) 12290–12297.
[14] G. Liu, J. Pan, L.C. Yin, J.T.S. Irvine, F. Li, J. Tan, P. Wormald, H.M. Cheng, Adv. Funct. Mater. 22 (2012) 3233–3238.
[15] Z. Wang, C.Y. Yang, T.Q. Lin, H. Yin, P. Chen, D.Y. Wan, F.F. Xu, F.Q. Huang, J.H. Lin, X.M. Xie, M.H. Jiang, Adv. Funct. Mater. (2013), http://dx.doi.org/10.1002/adfm.201300486.
[16] W.P. Qin, D.S. Zhang, D. Zhao, L.L. Wang, K.Y. Zheng, Chem. Commun. 46 (2010) 2304–2306.
[17] G.J. Feng, S.W. Liu, Z.L. Xiu, Y. Zhang, J.X. Yu, Y.G. Chen, P. Wang, X.J. Yu, J. Phys. Chem. C 112 (2008) 13692–13699.
[18] J. Wang, R. Li, Z. Zhang, W. Sun, R. Xu, Y. Xie, Z. Xing, X. Zhang, Appl. Catal. A Gen. 334 (2008) 227–233.
[19] J. Wang, T. Ma, G. Zhang, Z. Zhang, X. Zhang, Y. Jiang, G. Zhao, P. Zhang, Catal. Commun. 8 (2007) 607–611.
[20] L.N. Yin, Y. Li, J. Wang, Y. Zhai, J. Wang, B.X. Wang, G.X. Han, P. Fan, J. Mol. Catal. A Chem. 363-364 (2012) 265–272.
[21] L.N. Yin, Y. Li, J. Wang, Y. Zhai, Y.M. Kong, J.Q. Gao, G.X. Han, P. Fan, J. Lumin. 132 (2012) 3010–3018.
[22] W. Wang, N. Liu, Y.R. Du, Y.J. Wang, L.Y. Li, H. Jiao, J. Alloys Compd. 577 (2013) 426–430.
[23] M. Lidija, L. Vesna, A.M. Bojan, D.D. Miroslav, M. Olivera, Opt. Mater. 35 (2013) 1817–1823.
[24] L. Li, C.F. Guo, Y.Q. Chen, T. Li, J.H. Jeong, Mater. Lett. 95 (2013) 52–54.
[25] H.G. Yang, Z.W. Dai, Z.W. Sun, J. Lumin. 124 (2007) 207–212.
[26] C.J. Silva, R. Juárez, T. Marino, R. Molinari, H. García, J. Am. Chem. Soc. 133 (2011) 595–602.
[27] K. Maeda, M. Higashi, D. Lu, R. Abe, K. Domen, J. Am. Chem. Soc. 132 (2010) 5858–5868.
[28] J.C. Boyer, F. Vetrone, L.A. Cuccia, J.A. Capobianco, J. Am. Chem. Soc. 128 (2006) 7444–7445.
[29] B. Mitu, S. Vizireanu, R. Birjega, M. Dinescu, S. Somacescu, P. Osiceanu, V. Pârvulescu, G. Dinescu, Thin Solid Films 515 (2007) 6484–6488.
[30] H.J. Yan, J.H. Yang, H.J. Ma, G.P. Wu, X. Zong, Z.B. Lei, J.Y. Shi, C. Li, J. Catal. 266 (2009) 165–168.
[31] S. Du, L. Jiang, W. Zhang, X.R. Dong, Z.W. Dai, Opt. Commun. 284 (2011) 3593–3596.
[32] S. Du, J.X. Xu, X.R. Dong, J. Zhang, Z.L. Fu, Z.W. Dai, J. Lumin. 130 (2010) 872–876.
[33] J. Zhou, W.X. Zhang, L. Wang, Y.Q. Shen, J. Li, W.B. Liu, B.X. Jiang, H.M. Kou, Y. Shi, Y.B. Pan, Ceram. Int. 37 (2011) 119–125.
[34] X. Zong, H.J. Yan, G.P. Wu, G.J. Ma, F.Y. Wen, L. Wang, C. Li, J. Am. Chem. Soc. 130 (2008) 7176–7177.
[35] Q.J. Xiang, J.G. Yu, M. Jaroniec, J. Am. Chem. Soc. 134 (2012) 6575–6578.
[36] G.L. Chiarello, M.H. Aguirre, E. Selli, J. Catal. 273 (2010) 182–190.